

Measurement of Dynamic Rope System Stiffness in a Sequential Failure for Lead Climbing Falls

J. Marc Beverly, BS-EMS, M-PAS
Stephen W. Attaway, PhD

Abstract:

Background: Extended rock climbing leader falls resulting from sequential anchor point failures has led to much speculation regarding rope behavior. It has been postulated that an increase in stiffness (modulus) of the rope was likely responsible for subsequent anchor failures after a top point anchor failure. Understanding and forecasting the system response of a leader fall can help climbers gain understanding of the risk of sequential failure of rock climbing protection.

Methods: Using controlled methods with a standardized test mass, we performed drop tests on differing makes and models of rope from two separate manufacturers. High-speed digital video imaging at 500f/p/s was used in conjunction with multiple strain gauge impact force measurement to obtain force-elongation data during a multiple impact fall. Tracking software allowed for calculation of force verses system elongation through time during the falls.

A designed failure point was created for the top anchor point to simulate climbing protection failure, so that a subsequent impact force would be exerted on the following anchor point to mimic a real-world lead climbing scenario.

Conclusions: A leader fall is more complicated to define than many initially thought. Changes in system stiffness due to knot tightening appear to be greater than changes in rope stiffness. A residual velocity after the initial anchor point failure results in an increased effective fall factor for subsequent impacts. For equally spaced anchors of equal strength, this increased effective fall factor makes sequential failure highly likely.

OBJECTIVE:

A better understanding of how dynamic rope behaves during, and immediately after, a top point anchor failure in lead climbing orientation is needed. Understanding forces during a climbing fall is essential in preventing anchor failure due to high impact forces. Our objective was to measure the forces and system elongation during a typical climber fall, where one of the climbing protection pieces fails.

Some researchers have begun using computer simulation to gain a better understanding of the forces generated in a fall¹. An additional objective of this paper was to provide data that can be used to validate future computer simulation, such as the one on Petzl's² web site.

BACKGROUND:

Although climbing ropes have been made to meet standards set by the Union Internationale des Association d'Alpinisme (UIAA)^{3,4} the standards do not test or describe the characteristics created in many real-world climbing experiences. For

instance, not all climbers are 80kg⁵, and not all gear holds every fall by reason of poor placement, poor rock, or a combination of factors. How rope behaves after a fall can also vary⁶.

Our testing goal was to measure what happens to the dynamic rope properties in handling a second shock load immediately after the initial point of protection fails. Some have witnessed lead climbers pulling out an entire pitch of anchor points, resulting in a ground fall⁷.

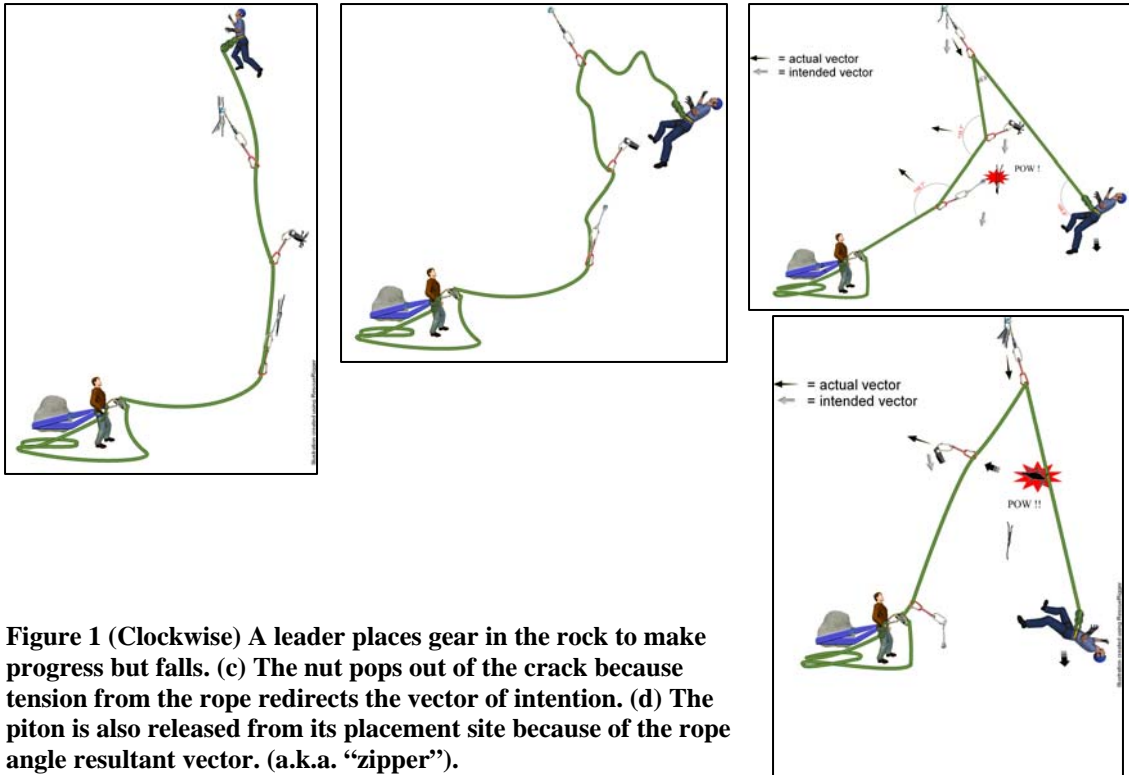


Figure 1 (Clockwise) A leader places gear in the rock to make progress but falls. (c) The nut pops out of the crack because tension from the rope redirects the vector of intention. (d) The piton is also released from its placement site because of the rope angle resultant vector. (a.k.a. “zipper”).

Here, we will define some terms for describing sequential failure. The *Descriptive Fall Definitions* defined below assume the following scenario: a lead climber has placed one or more directional anchor points designed to hold a vertical fall. Sequential failure is a different scenario than the “zipper” effect^{8,9}. Within the rock climbing community, the terms “zipper”, “zip-out”, and “unzip” all relate to the same concept. However, the definitions are loose and, generally, all these terms mean that the anchor protection points have failed. Climber lingo does not describe the method in how failure is initiated or continues.

A *zipper* is defined as when a lead climber loads a rope such that the angle of the rope from the belayer places an outward pull on the protection, resulting in popping out pieces from the bottom to the top. These types of zipper failures are usually the result of unexpected outward/upward forces being placed on lower anchor points (See Figure 1).

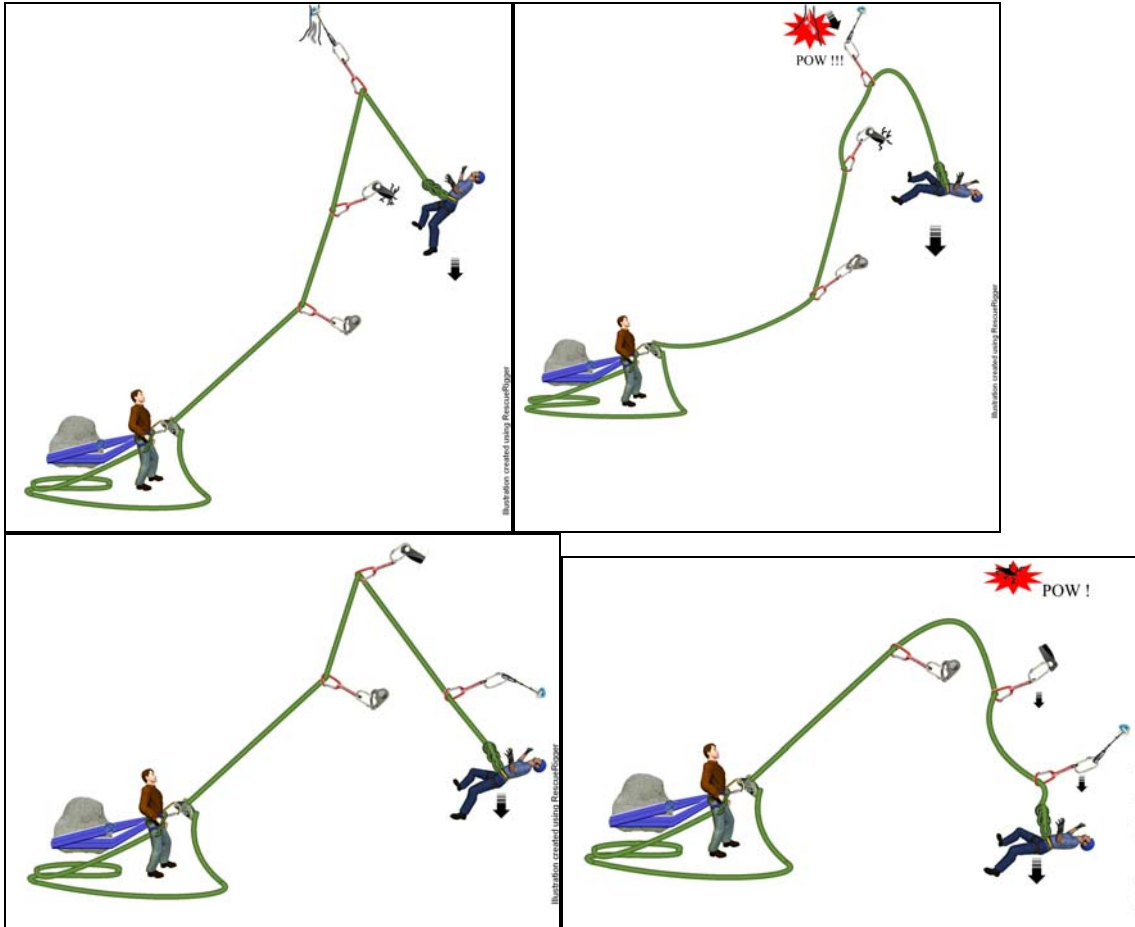


Figure 2 Sequential Failure (S.F.) (a.k.a. “un-zipping”) left to right, top to bottom. The cam fails, the climber continues to fall, weights the piton, then pops out the piton.

A *un-zipper* is defined as when a climbing protection fails one-by-one, from the top to the bottom, hereafter referred to as sequential failure (SF) (see Figure 2) In SF, if all the protection points pull out, the result is often a ground-fall.

Some sources state that, “if your unfortunate choice is between questionable protection or none at all, by all means place something¹⁰.” If rope properties change greatly after a shock loading, perhaps questionable protection that fails may actually make the situation worse and contribute to overall higher impact forces on subsequent pieces during SF.

APPROACH:

Hypothesis:

The modulus of a dynamic rope increases after absorbing an impact force when a top anchor point fails, such that the resulting impact force on the subsequent anchor point is higher than the initial impact force. The cause of increasing stiffness of the rope is likely due to permanent deformation of the dynamic rope, the inability of the rope to return to its initial state due to a lack of time to rebound from the primary impulse, or a combination of these or other factors.

Some of the unknowns at the start of testing include:

- How much energy is removed from the system by a piece pulling out?
- Can a fall factor be defined for the second impact?
- On the second impact, the fall distance and initial velocity are unknown. Will the second impact be greater than the first impact?
- Will there be a significant increase in rope stiffness?

The null hypothesis is that there is no significant difference in impact forces seen by the two anchor points being monitored, and there should not be a notable increase in dynamic rope modulus resulting in higher than expected impact forces on subsequent anchor points.

Static based observations show that a finite amount of time is required for the rope to relax back to the near-initial state. Climbing ropes use highly twisted yarns confined by a braided sheath to allow them to undergo very large elongation and absorb fall energy. Kernmantle ropes have a high strength inner core (kern) that is covered by a braided (woven) outer sheath (mantle). The inner core of high-stretch kernmantle dynamic ropes typically consists of several highly twisted yarns.

As the rope is stretched, the outer sheath will tighten much like a Chinese finger trap, thereby “entrapping” the core. This tightening will provide a confining pressure on the inner bundles of twisted yarns. The confining pressure generates high internal friction forces that dissipate energy as the fibers slip past each other and untwist and lengthen.

Frictional resistance to internal fiber slipping occurs in both loading and unloading. Once entrapped by frictional forces, the fibers will respond without slippage until the frictional forces are exceeded. Small changes in force/elongation through unloading from the virgin load curve do not result in fiber slippage, and the slope of the force-elongation path is much stiffer. This effect appears to hold only for small unloads and reloads. For larger unloads, reduction in tension allows fiber slip in the reverse direction and result in force-elongation curve relaxing to a lower slope. The rope modulus during a small unload/reload cycle of load/reload does not appear to be function of the rope tension.

Once the tension in the rope is reduced below a critical value on unload (i.e. the back-slip tension), the internal frictional force relaxes enough to allow the fibers to slip relative to each other and contract, which will reduce the apparent rope stiffness. The rope appears to auto anneal once the entrapping pressure is reduced. If the tension is completely removed from the rope, then the internal pressure created by the sheath will drop to zero. Given time, all of the fibers can relax back to their near-initial state.

TESTING

Test Mass: We used both a 90kg mass for drop testing. The test mass was manufactured using plated steel for adjustability, a large shackle as a connection point, and a quick-release trigger.



Figure 3: A 90 kg (200 pound) test mass with load cells in line and freefall drop zone.

Configuration

A rigid wood tower was utilized for drop testing. All drops were configured to produce compression on the beams as to keep any deflection to an absolute minimum. Deflection of the tower was determined to be negligible by photometric measurements of drops prior to actual testing.

The angle between the anchor and the first piece was 30 degrees to keep in the flavor of the UIAA drop tests. This configuration is representative of where an actual belayer would place themselves in an actual climbing scenario, out of the way of a leader fall.

Adjustment of the distance between the anchor and the first piece was used to establish the fall factor.

A combination of three load cells was used to measure the entire force on the system. A Microstrain data logging system recorded the forces of each individual point in the anchor system at 2,000 cycles per second. The force on the test mass was calculated as the resultant force from the total force in the system. Velocity and other parameters of the

test were measured through standard photometric techniques. The data logging system triggered the camera to provide synchronization with the load cells.

Displacement of the rope was measured by high speed video at 500 frames per second with a 512 by 1024 frame. The field of view was approximately 10 meters in height, which resulted in a pixel accuracy of roughly 1 cm.

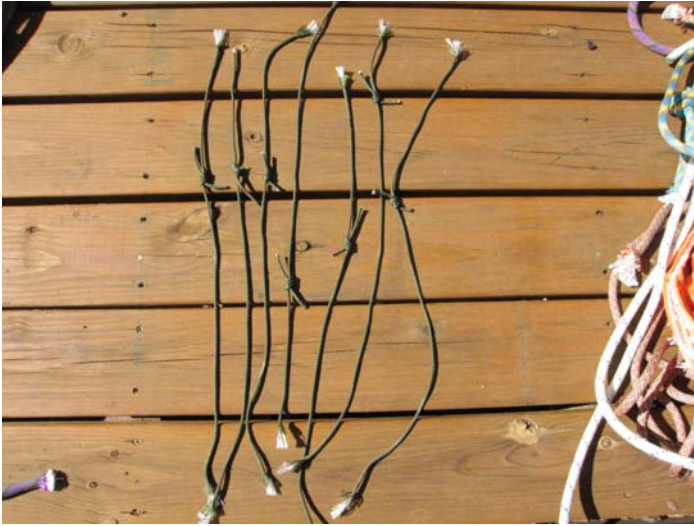


Figure 4: Examples of dynamically tested failures.

The designed failure was determined from static tensile testing to fail at roughly 7-8kN force, near the “average” strength of a piece of rock¹¹ or ice¹² protection. The designed failures used in our drop testing failed consistently at 7-8kN (Figure 4). The range of strength of any real anchor point can vary widely depending upon many factors. The goal here was to have a representative failure typical of the average loads seen by possible failed rock climbing protection. The designed failure was incorporated into the system at the “second top piece” (second anchor point placed by a would-be leader).

To control for coefficient of friction¹³ and a possible confounding variable, the same type aluminum carabiner was used for all tests and throughout the system: a locking Petzl Attaché.

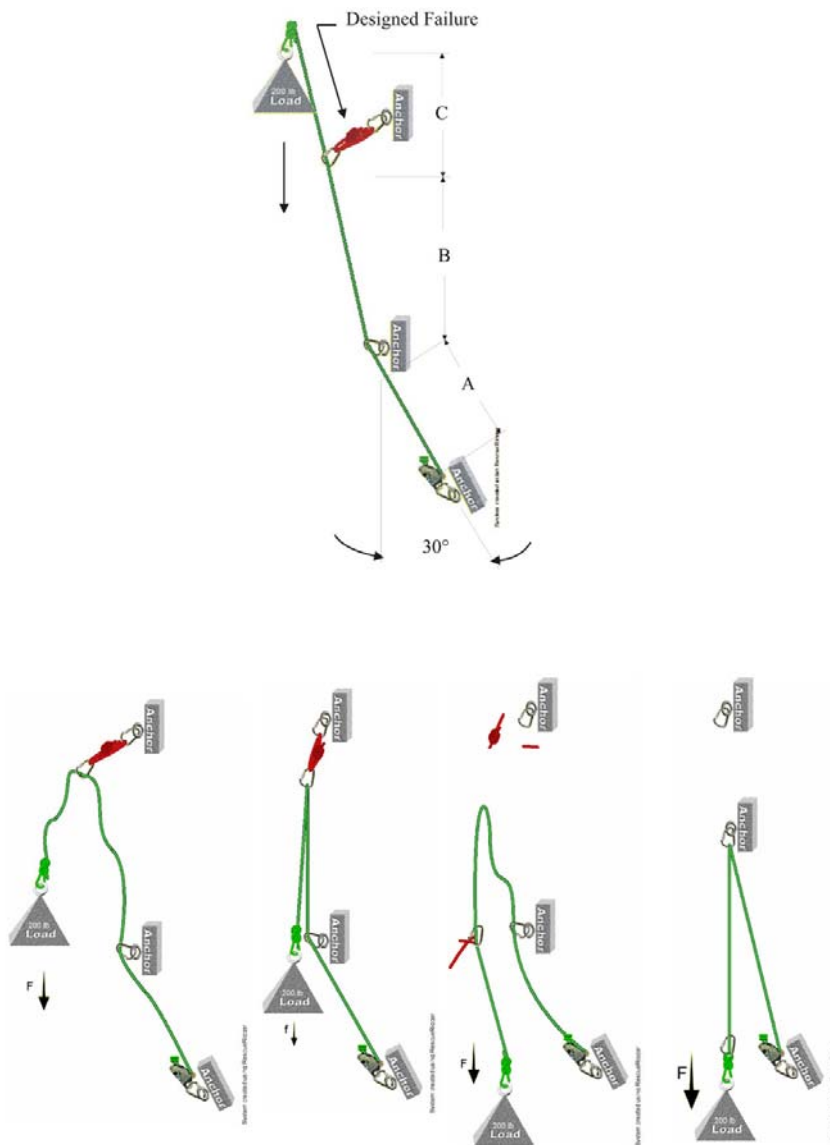


Figure 5 A two impact fall used to simulate the failure of rock climbing protection. The bottom anchor represents the belayer location. The climber is represented by a 200 lb mass. The second top anchor is designed to fail at a predetermined load (actual Fall Factor dimensions listed in subsequent tables).

Weather conditions at our testing facility at 35.11° N latitude in Albuquerque:

Temperature ranged at our outdoor facility from 58F° to 79F° (14°C to 26°C) with clear blue skies and no wind. Average humidity throughout the testing ranged at 10-20%. Some manufacturers do further testing in cold and/or frozen conditions. We suspect that extrapolation can be made to any of our soft-goods testing to increase impact forces by approximately 10-15% on average¹⁴, so we did not conduct these tests with cold, frozen, or wet rope.

The test setup was based on the two impact fall shown in Figure 5. A figure-8 knot was used to attach the rope to the mass. A Grigri with stopper knot was used to attach the rope to the belay anchor^{15, 16}. The lengths between anchors (A, B, and C shown in Figure 5) varied depending on the desired test conditions.

RESULTS:

The dynamic forces from a fall depend on how the rope elongates under load. If the rope is viewed as a spring, then the force will be proportional to the amount of stretch in the rope. For climbing ropes, the following formula as been found to be reasonably accurate:

$$F = K\delta \tag{1.1}$$

where F is the force in the rope, K is called the stiffness of the rope, and δ is the displacement of the rope from its unloaded length.

The stiffness of the rope, K, depends on the length of the rope. Short ropes are very stiff, and long ropes are less stiff. The rope stiffness can be computed as:

$$K = \frac{M}{l} \tag{1.2}$$

where M is defined as the rope modulus and L is the rope length. The rope modulus is computed from the stretch in a rope:

$$M = \frac{F}{\varepsilon} \tag{1.3}$$

The stretch is simply:

$$\varepsilon = \frac{\delta}{l}. \tag{1.4}$$

Ideally, one would like to measure the change in length per unit length of the rope for a given load. This measurement was not practical due to the limited resolution (1 cm) of the photometric system. Friction, knot tightening and anchor movement contribute to the overall system stiffness. The system modulus is defined as

$$M_s = \frac{\Delta F}{\varepsilon_s} \tag{1.5}$$

where the change in the force is the force measured at the top anchor point. The elongation is

$$\varepsilon_s = \frac{(l - l_0)}{l_0} \tag{1.6}$$

The length, l , in Equation 1.6 will reflect the system stiffness if it includes the stretch in the knots.

For the purpose of testing, we computed the loading system modulus using the force and rope length at 2kN load and the force and rope length at the maximum load.

$$M_s = \frac{F_{max} - F_{2kN}}{l_{max} - l_{2kn}} l_0 \quad (1.7)$$

Figure 6 shows a load-elongation data measured from repeated single falls on the same rope. In this base line test, no anchor failures occurred. The repeated impacts appear to stiffen the rope system. The system stiffness increased by almost 70% between these two drops. Knot stiffness is an important part the system stiffness. The plot shows the force as a function of elongation for the rope system. The loading portion of the impact shows an almost linear force-elongation relation.

The system modulus is the tangent to the force-elongation curve and may change as a function of rope stretch. As can be seen on the plot shown in Figure 6, the unloading stiffness is much greater than the loading modulus. Static tests that unload by 20% of the load will reload with the same modulus as the unloading curve.

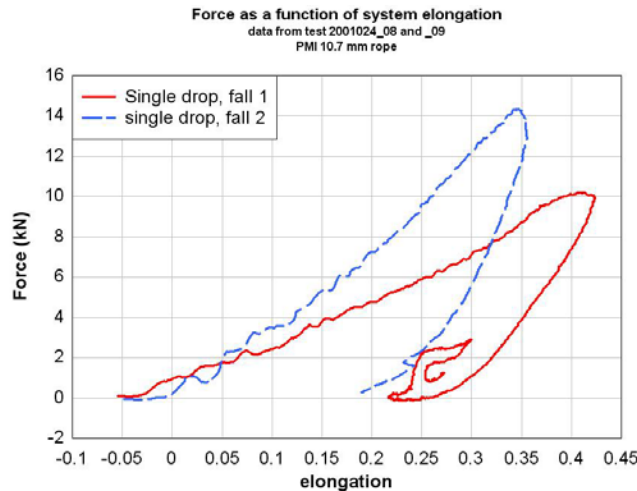


Figure 6 Force as a function of elongation for the same rope dropped twice.

Figure 6 shows the measured force and displacement as a function of time for a two part impact. The blue lines show the velocity and the displacement as measured using tracking points in high speed video. The velocity during free fall was a linear function of time (as expected by theory). From $t=0$ to 0.8 ms, the mass is in free fall. The first impact occurs at $t=0.8$ to 1.0 ms. During this time, the top anchor reaches a peak force of 7.5 kN, with the belay anchor reaching a peak force of 3 kN. After anchor failure, the mass accelerates from 1.0 ms to 1.2 ms. At $t=1.2$ the second impact on the lower anchor starts. The peak force on the second anchor was 8.5 kN, with a peak force on the belay anchor of 3.5 kN.

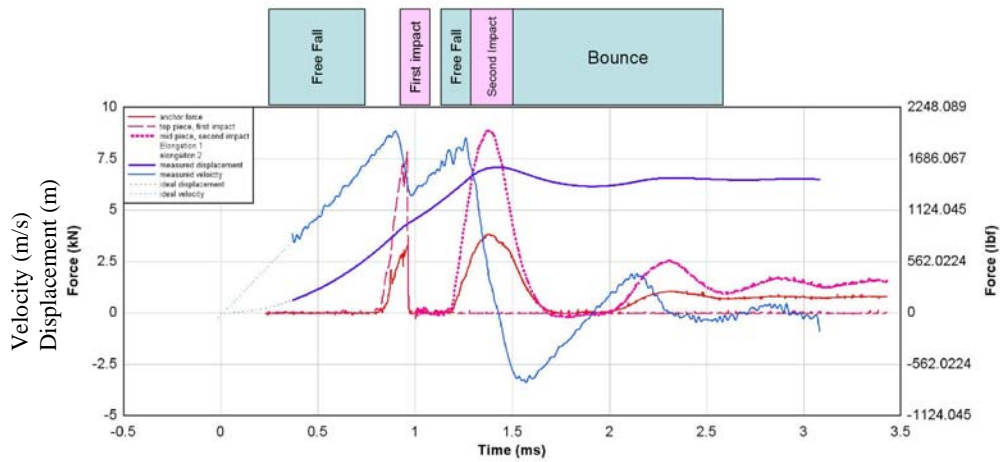


Figure 7 Force as a function of time for two impacts.

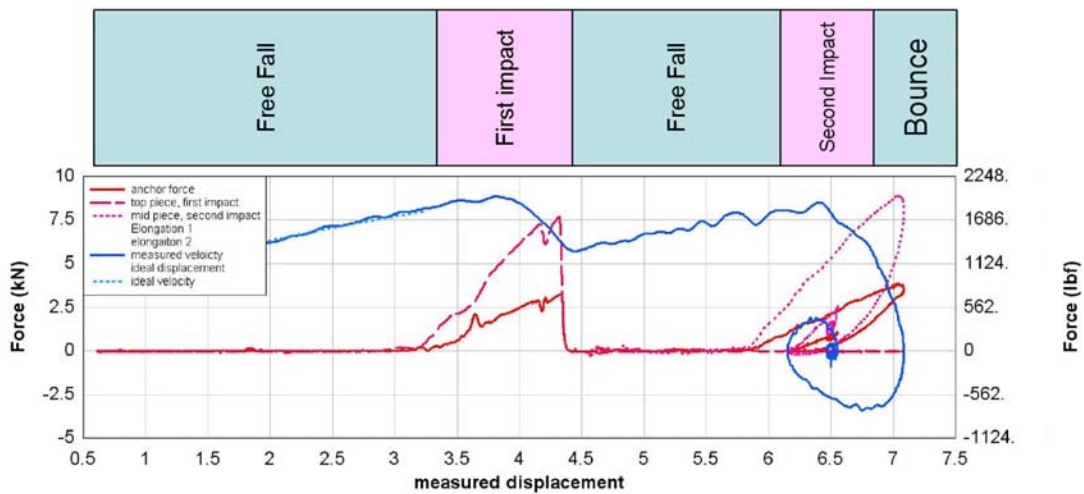


Figure 8 Force as a function of displacement for a two impact fall.

The force was measured at three different locations using synchronized load cells. During the first impact, the force was measured at the anchor point and the top point. The peak force at the top point was 7.5 kN. The peak force at the anchor point was 3.0 kN.

Figure 8 shows a plot of the force and velocity as function of displacement for a two impact fall. The slope of the force-displacement corresponded to the system stiffness.

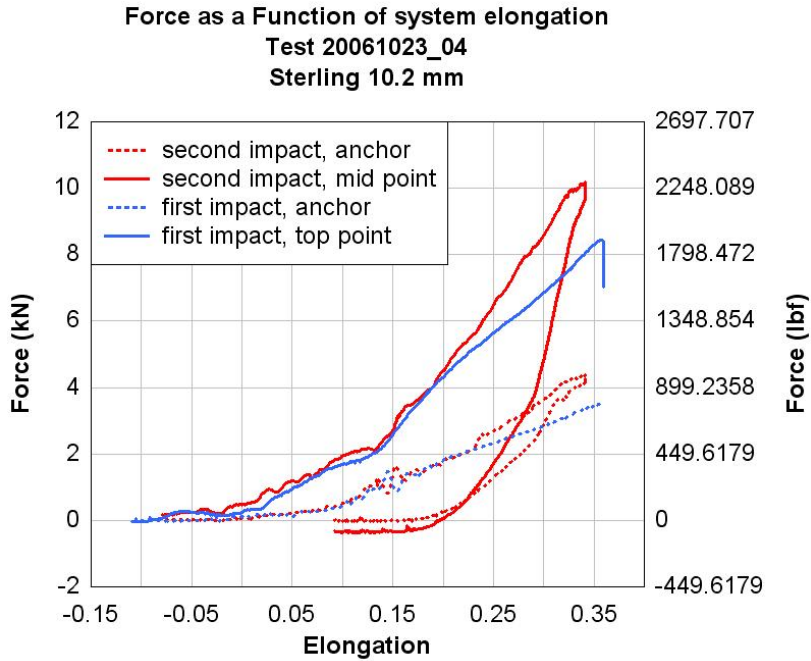


Figure 9 Force as a function of elongation for a two impact fall.

Figure 9 shows a plot of force as a function of elongation for a two impact fall. Some observations:

- Initial system stiffness is the same
- Stiffness on the second impact increases after 20% elongation
- Total system force at 28% elongation is 25% higher

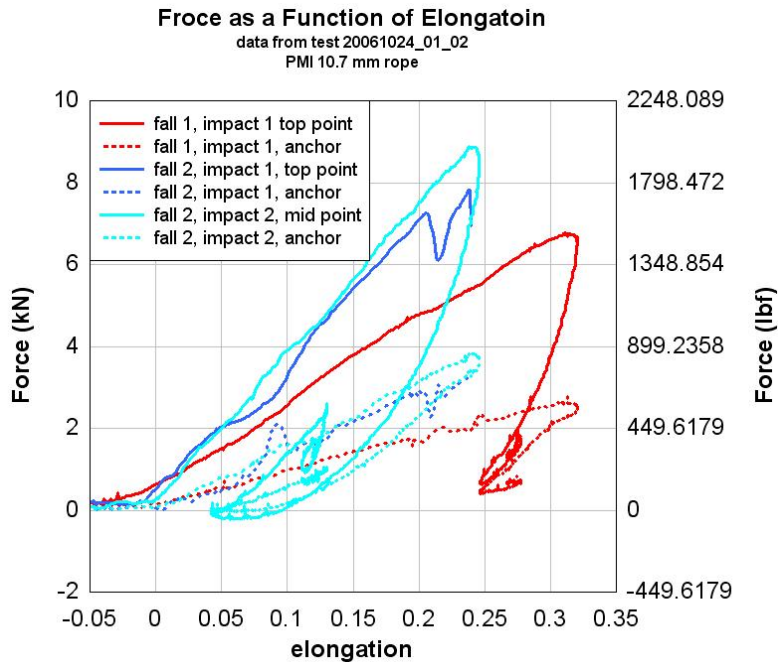


Figure 10 Force as a function of elongation for two falls.

Figure 10 shows the force as a function of elongation for two drop tests. The same rope was used in two different drop tests without knot retying. The first drop test had only one impact. The second drop used a programmed failure at 7.8 kN and generated two impacts. Thus, a single rope was impacted three times. The plot shows the force at both the top points and the belayer anchor point as a function the system elongation. The system elongation is defined as the change in length of the distance between the mass and belay anchor point divided by the initial length of rope between the mass and the anchor point.

Knot tightening reduced the system stiffness for the first impact; this phenomenon was reflected in subsequent tests. Stiffness of the first impact on the second fall (dark blue) is greater than the first impact (red). The stiffness on the second impact of the second fall is not much greater than the stiffness of the first impact on the second fall. The change in stiffness appears to be a function of knot tightening, and not a function of rope mechanics.

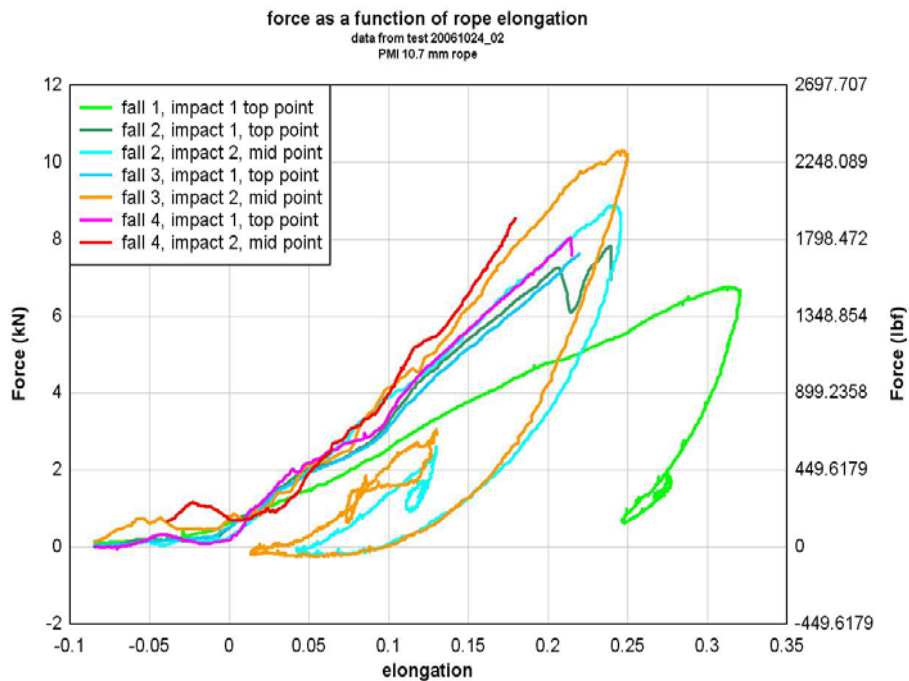


Figure 11 Force vs. elongation for four drop test on the same rope. In the first drop only one impact occurred. In drops 2-3, two impacts were simulated.

Figure 11 shows the results from the two tests discussed in Figure 10 with two additional two-impact drops.

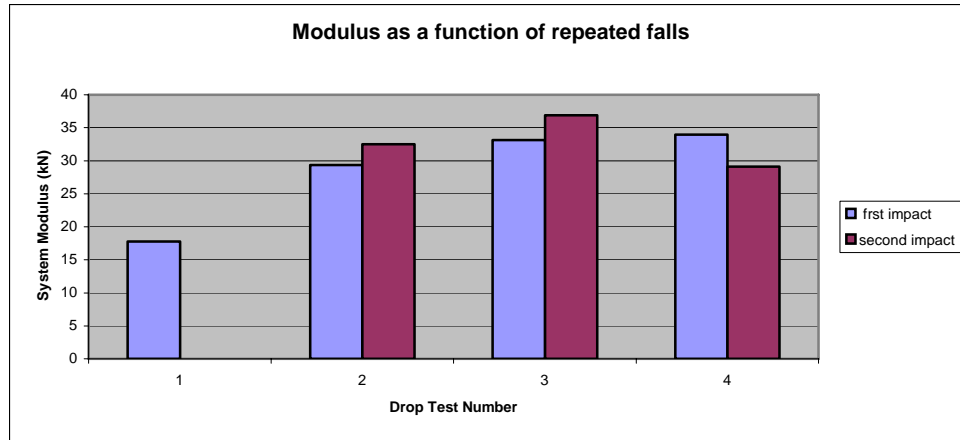


Figure 12 System modulus as a function of number of impacts.

Figure 12 shows that the system modulus does not always increase with each impact⁶. It also shows that the modulus for the second drop may be lower than the system modulus of the first drop.

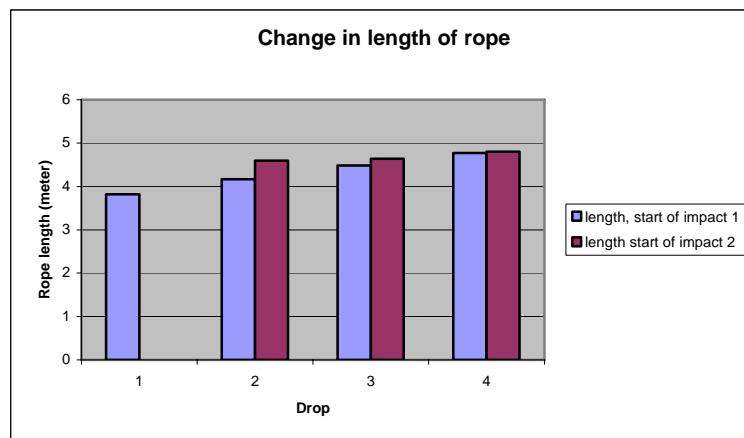


Figure 13 Change in rope length as a function of test drop.

Figure 13 reports the change in rope length with each test. Consistently, there was a slight increase in length with each drop. Table 1 summarizes the test data collected from four drops.

Table 1 Summary of test data.

Test	Rope Length (m)	Fall Factor	Modulus (kN)	Anchor Force (kN)	Belay Force (kN)	Climber Force (kN)	belay/climber
T 01-2	3.82	0.60	17.76	6.78	2.60	4.18	0.62
T 02-1	4.17	0.77	29.35	7.83	3.25	4.58	0.71
T_02-2	4.59	0.59	32.49	9.74	3.86	5.88	0.66
T_03-1	4.48	0.77	33.14	8.07	3.39	4.68	0.72
T_03-2	4.64	0.73	36.91	10.28	4.52	5.76	0.78
T_04-1	4.77	0.81	33.95	8.11	3.38	4.73	0.71
T_04-2	4.80	0.83	29.12	8.68	3.39	5.29	0.64

Fall Factors

Fall factors are often used to communicate the severity of a fall. The fall factor is defined as the free fall distance divided by the initial length of rope in service. For the first impact, the fall factor can be measured from the initial conditions. For the second impact, computing the fall factor is more complicated because the mass has an initial velocity at the start of the fall. The equivalent fall factor can be computed by computing the height from which the mass would have to fall to generate the residual velocity after the first piece of protection fails.

The fall factor for the second impact can be computed given the equations of motion for a free falling mass under gravity load, g , as:

$$v = \int g dt \quad (1.8)$$

$$y = \int (v_0 + gt) dt \quad (1.9)$$

High speed video can be used to measure the time and location of the falling mass at two points after the first piece has failed, the velocity at the a given location can be computed as

$$v_1 = \frac{(y_2 - y_1) - \frac{g}{2}(t_2^2 - t_1^2)}{t_2 - t_1} \quad (1.10)$$

The time at which the velocity will be zero is:

$$t_0 = \frac{v_1}{g} \quad (1.11)$$

The equivalent height of the fall can then be determined as:

$$h = y_2 - \frac{g(t_2^2 - t_0^2)}{2} \quad (1.12)$$

The equivalent fall factor for the second impact can then be computed as:

$$FF = h / L_{rope} \quad (1.13)$$

Figure 14 shows the fall factors corresponding to the test shown in Figure 11 and Figure 12. In the first drop, the forces were not great enough to snap the designed failure, so only one fall is reported. For drop tests 2, 3, and 4, the program failure resulted in a two impact fall. Had the same fall distance only been arrested by the bottom piece of protection, the fall factor would have been $FF=1.42$. Absorbing energy in the first fall and failure of the top point resulted in a reduction of the fall factor compared to what the fall would have been if a single impact had occurred.

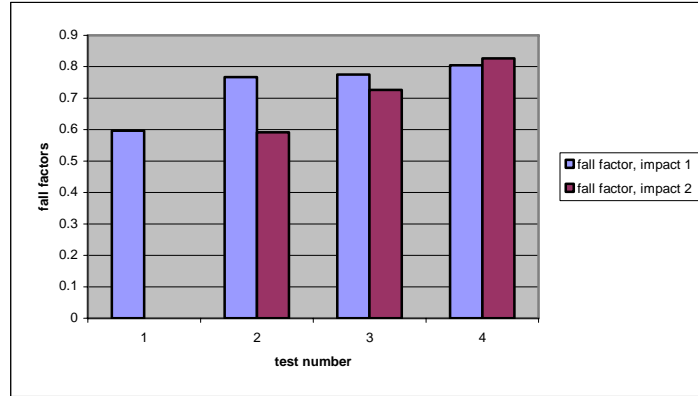


Figure 14 Fall factors for a set of four drop test.

On the second impact, the fall distance and initial velocity are unknown. Computation shows that for the particular set of falls that we studied, the fall factors for each impact was almost equal. How the fall factors distribute between impacts will depend on the geometry of the fall and on the forces required to fail the protection. In general, the fall factors will not be equal.

Static vs. Dynamic Rope mechanics

Figure 15 shows the force as a function of elongation for the same rope used in the drop test. Three slow pull tests were performed. The pull rate was over 60 seconds. A new rope was loaded to an elongation of 35% and a load of 6.2 kN. The load was quickly released and reloaded to show the unload modulus. After unloading, the rope was 8.2% longer.

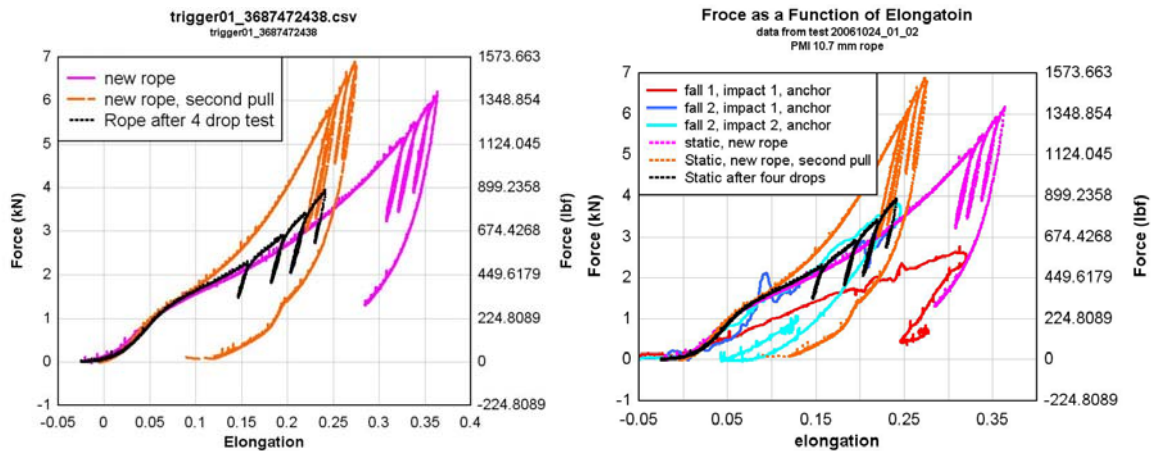


Figure 15 and Figure 16 Static results compared with the force at the belay anchor for dynamic drop test.

A second slow pull test on the same rope showed a marked increase in the rope modulus. After unloading, the rope had 12% elongation at zero load. Also shown in this plot is a slow pull test on the same rope used in the four drop test discussed above. The rope was

allowed to set for 9 months on a shelf in a garage (and otherwise out of the elements in Albuquerque, New Mexico) between the drop test and the static pull test.

Figure 16 shows the results of the static pull test with cyclic loading compared with the belay anchor force as a function of system elongation for the first two drop tests described in Figure 10. Some caution should be used in comparing the data set presented in Figure 16. The static test results measure the rope modulus. The dynamic results show the anchor force at the belay as a function of system elongation. We could have plotted the force on the mass, which would have been about 30% higher, or we could have taken the weighted average of the rope on the belay and climber side. The significant point in these plots is that after the initial knot tightening impact, the system modulus in the dynamic test is almost constant. The static test shows that there is considerable stiffening over two loading cycles.

Our testing has shown that the unloading and reload process in a dynamic event, with a rapid failure and subsequent reloading, is very different from the static event described in Figure 16. The rapid unloading from an anchor failure can briefly drive the rope into compression. Evidence of this dynamic compressive force was captured, as shown in Figure 17, where a dynamic buckle in the rope forms just after the top piece fails. The buckle forms due to dynamic snap-back driving the rope into compression. The high strain energy in the rope at the time the top piece fails results in very rapid unloading of the rope, much like the rapid unloading of a rubber band. Just as a rubber band can snap back and impact your fingers with a sting, the stored energy in the rope results in a very dynamic event. High speed video was able to capture the buckle formed in the rope during snap-back.



Figure 17 Buckling of rope during unload snap-back.

Driving the rope into compression removes the compressive load from the outer sheath and allows the rope fibers to return to their near-initial un-stretched length. Unlike static testing, or a climber who merely falls and hangs on a piece of gear and then lowered to

the ground, no delay time is needed for the rope to return to its “original” state between impacts on the anchor points.

Static vs. dynamic ropes used for belay

Recall that the system stiffness depends on the combination of the rope stiffness, knot stiffness, and frictional effects. The rope stiffness is an inverse function of the rope length, as described in Equation 1.2. Increasing the length of the rope should reduce the overall stiffness of the belay system. Some rescue teams have suggested that a long static rope can be used as a belay.

Figure 18 shows a comparison of a long static belay to a shorter dynamic belay. It is well known that the modulus of a static rope is much greater than for a dynamic rope. Static ropes also generally do not follow a linear load displacement path.¹⁷ Even when the force is not a linear function of rope stretch, the system stiffness will still be inversely proportional to rope length (see Equation 1.2). If the rope is long enough, then the decelerations from stopping a climber fall may be low enough to be acceptable.

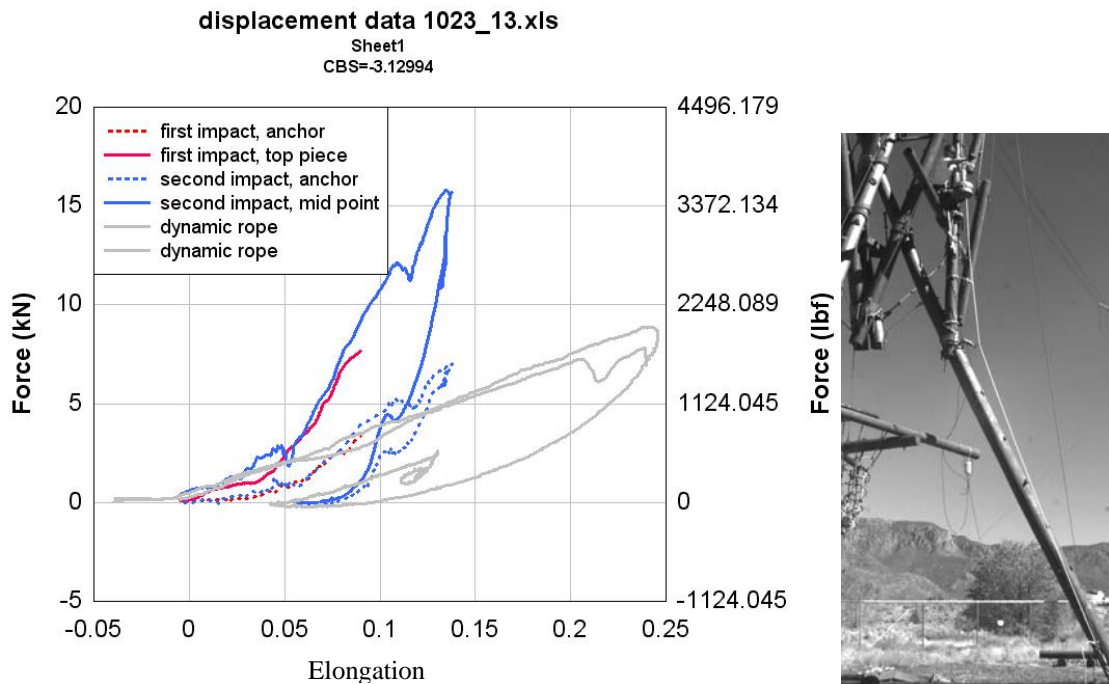


Figure 18 Two impact drop using “long” static rope.

Even with the “long” static rope, the force in the two-impact drop was almost twice the force that resulted from impacts on dynamic rope. Clearly, our rope was not long enough. This scenario could easily be encountered in tower climbing or tower rescue.

Table 2: Fall factors and peak forces at top most anchors for static rope test. (new 11mm PMI 5% stretch static nylon rope)

Test	Rope length (m)	fall factor	Modulus (kN)	Peak Force (kN)
13-1	8.92	0.37	143.36	7.1
13-2	9.75	0.59	177.34	15.1

We performed only one test on a static rope in lead climbing configuration. We found that, with a fall factor of $FF=1$, we were able to produce impact forces that would likely cause significant morbidity and mortality. However, with lower fall factors of less than $FF<0.3$, it may be reasonable¹⁸. A low fall factor may mean that an anchor will need to be located far away (>10m) from the structure. Knowing how to rig a “safe residual” of rope may be difficult since static rope used in the workplace is rarely brand new.

Table 2 shows the summary for the two impact drops on static rope. The fall factor for the second drop was not reduced as much when compared with the dynamic ropes. The energy absorbed during a drop is equal to the area under the force-displacement curve. The increase in stiffness of the static rope reduces the energy absorbed and results in a higher residual velocity compared to the dynamic rope.

The tests on “long” static ropes presented here are for illustrative purposes and should not be considered conclusive. The test used a static belay device that does not allow for rope slippage through the belay anchor. A dynamic belay device will clearly change the outcome for “long” static belays.

Estimating sequential failures

Given a set of anchor placements and anchor strengths, a rough estimate of the potential to unzip the line of protection can be computed based on potential energy and the work done on the falling mass during each impact.

The kinetic energy from a fall of height h will be:

$$KE = mg(h + \delta) \quad (1.14)$$

where δ is the additional displacement due to the stretch in the rope.

For an anchor that fails at a force of F_{anchor} , the work done on the mass at the time the failure occurs will be:

$$W = \frac{1}{2} F_{mass} \epsilon l_T \quad (1.15)$$

where F_{mass} is the force acting on the mass, ε is the *system* elongation at anchor failure, and $l_T = l_1 + l_2 + l_3 + l_n$ is the total length of the rope with l_n the length between each piece of protection. Equation 1.15 assumes a linear relation between force and elongation. This generally holds for dynamic rope, but is not accurate for static rope. For static rope, a second order fit for force as a function of elongation can be used to compute the work from the area under the force/displacement curve.

The force on the climber side of the rope will be higher than the belay side of the rope due to friction. The ratio measured from our test showed

$$F_{mass} = RF_{anchor} \quad (1.16)$$

with approximately $R = 0.6$ to 0.7 . Here we use $R=0.6$.

The first anchor will fail if the KE is greater than the work done when the anchor force reaches its load limit.

$$KE_1 = mg(2l_1 + \varepsilon l_T) > \frac{1}{2} RF_{anchor} \varepsilon l_T \quad (1.17)$$

Note that ε is the system elongation at failure and F_{anchor} is the anchor failure force, both of which can be estimated from the plots shown in Figure 10. Just after failure of the first anchor, the KE in the falling mass will be:

$$KE_2 = KE_1 - \frac{1}{2} F_{mass} \varepsilon l_T \quad (1.18)$$

The velocity just after the anchor failure will be:

$$v_2 = \sqrt{\frac{2KE_2}{m}} \quad (1.19)$$

This initial velocity can be treated as an equivalent fall height given by

$$h' = \frac{v^2}{2g} \quad (1.20)$$

At the time of the second anchor impact, the mass will have fallen through an equivalent height of $h_2 = h' + 2l_2$. This equivalent height can be used to compute an equivalent fall factor for the second impact, with the steps above repeated for each subsequent impact.

If anchors are placed at equal spacing and have equal strength, then the addition of an equivalent fall height as a result of residual velocity insures that the fall factor on the second impact will be higher than the first. This means that if the first anchor fails, the rest of the anchors will fail. ***If the top point fails due to fall from a height equal to the anchor spacing, then sequential failure is almost certain for equally spaced, equal strength anchors.***

For unequal spacing and unequal strength, estimating if a line of anchors will unzip is more complex. Using the information from our drop testing, and Equations 1.16 through 1.20, a crude forecast for the likelihood of sequential failure is possible.

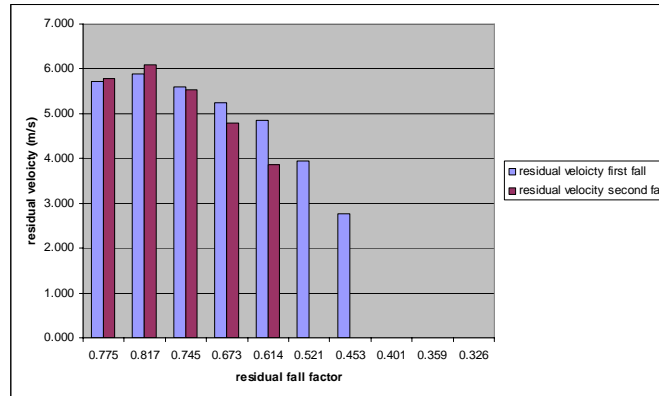


Figure 19 Residual velocity vs. initial fall factor for a lead climber weighing $m=90\text{kg}$ in sequential failure on a dynamic rope with at 1.7 and 0.92 m length between climber, top point, and anchor.

Figure 19 reveals the high likelihood of a sequential failure event once a top point failure occurs. The plot shows the predicted residual velocity after each impact. A zero residual velocity indicates that the anchor will not fail. In the plot shown, it was assumed that the climber protection was spaced the same as in test T 02-1 shown in table 2. This test had an initial length of 1.7 meters above the first anchor and 0.92 meters between the top and mid anchor. The calculation shows the effect of increasing the distance between the belay and the mid anchor, which adds more rope to the system, thus, reduces the fall factor (x-axis). In this case, with the parameters of our testing (90kg mass parameters as described earlier), sequential failure for the subsequent impact will likely occur until the rope length is increased to reduce the initial fall factor to below $FF < 0.5$. Below a fall factor $FF < 0.4$ the top anchor does not fall.

The transition between arresting the second fall and unzipping is represented by the absence of residual velocity on the second impact at $FF=0.5$ (i.e. the second anchor held). For initial fall factors above $FF > 0.5$, energy is absorbed from the top anchor failing; however, the falling mass will likely fail the second anchor. Changing the rope stiffness, climber mass, or anchor strength will change the outcome. (See Figure 20)

Figure 21 shows simulated falls on a brand new 11mm static rope. The graphs show the results for 7.8 kN anchors and 22 kN anchors. The static calculations assume the force acting on the mass take on the form:

$$(1.21) \quad F = a\varepsilon^2$$

where $a = 645$ was determined from a fit of test data shown in Figure 18. The calculations indicate that both top and mid 7.8 kN anchor failures would be likely even when the fall factor is reduced to $FF=0.1$ (a rope length $L > 35$ m). **(Never expect an ice anchor to hold a leading climbing fall on a static rope).**

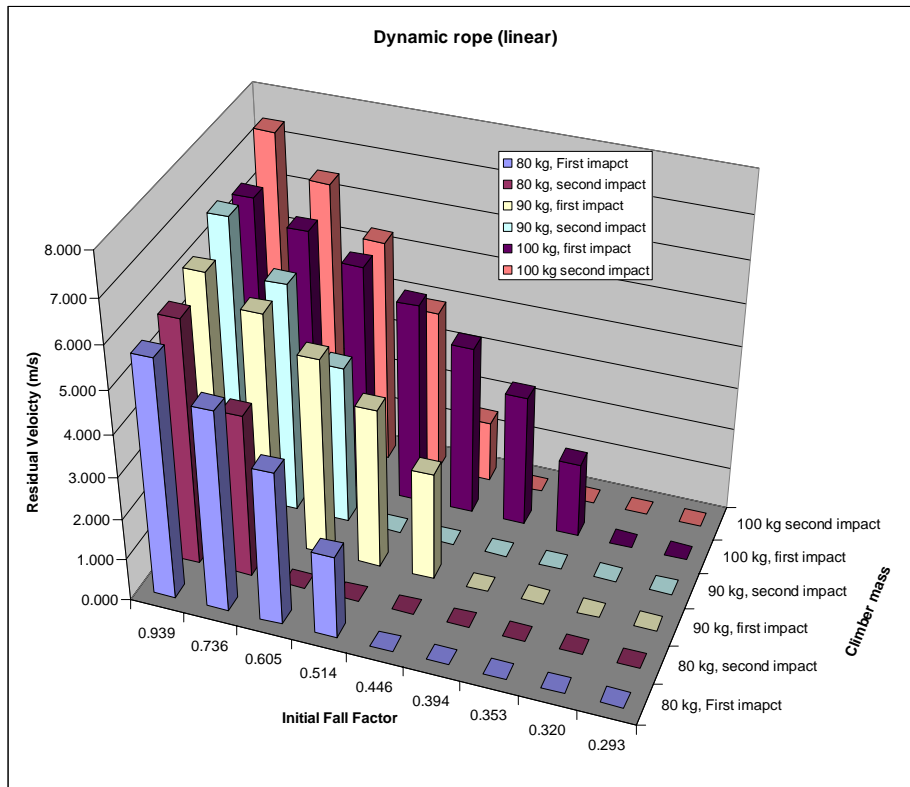


Figure 20 Effects of climber mass on the likelihood of sequential failures.

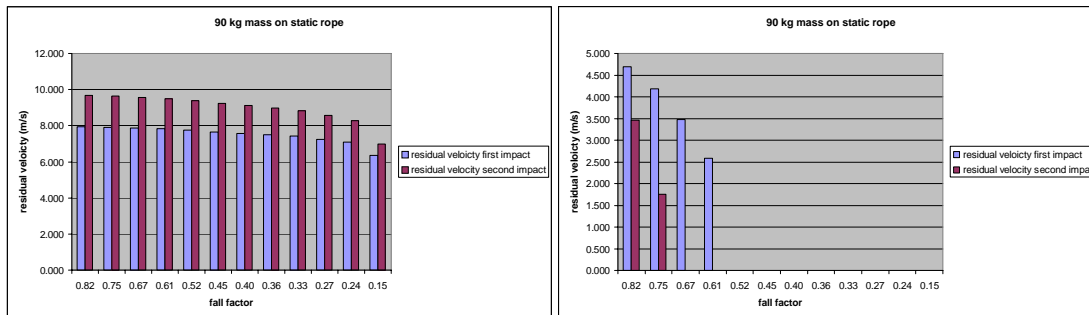


Figure 21 projected sequential anchor failures when leading with a static rope (a. 7.8 kN anchor, b. 22 kN anchor)

Figure 21 show the results for a 22 kN anchor. Even with the stronger anchor, the safety margin is narrow indeed. For initial fall factors greater than $FF > 0.5$ ($L > 6$ m), with all anchor points assumed to be 22kN, the simulation predicts failure of the top-most anchor point. For falls on static rope with $FF > 0.7$, expect sequential failures. Forces generated in fall factors of $FF > 0.5$ are high enough to fail some carabiners. These calculations assume new rope and no slippage at the belay.

Unfortunately, forces generated in fall factors of $FF > 0.35$ on static rope may be high enough to cause significant morbidity or mortality, even if the fall is in clean air and the anchors hold. Speculatively, this significant morbidity likelihood could be the cause of

tree-stand death, as these fall factors are at or near $FF=1$. Disruption of vital organs causing non-immediate co-morbidities is possible, regardless of harness type¹⁹.

RECOMMENDATIONS:

In consideration of anchor placements when lead climbing, we have the following recommendations that climbers should consider when placing their own protection anchor points for progression.

We were able to make accurate measurements of the system stiffness and show that knots play an important role in system stiffness. The figure-8 follow through knot absorbs an equivalent of nearly 1.5 m (5 feet) of rope for the first impact force. After that, the knot is “hardened” and has less absorptive ability. Some climbers have theorized this and make it a general practice to re-tie their knot after every fall. Although not of practical use on bolted sport routes, this could have major consequences when falling on questionable anchor points.

If the anchor arresting the fall is dubious, consider being lowered to the ground after a fall and switch ends of the rope. This will accomplish many things. Mentally, it will facilitate time to re-gather and consider an alternate approach. It will also allow any subsequent fall to be held by rope that has not been “recently” stretched. More importantly, it will allow the knot to be retied, which will lead to a decreased impact force.

Except for knot tightening, we did not observe rope hardening in the *two impact* drop. The rapid unloading after an anchor fails appears to reset the rope to its initial state. Testing on two impact drops showed that failing a piece of climbing protection absorbs energy and reduces the total fall factor. In the example studied, about half of the energy was absorbed on the first impact. While our simulated anchor failures in this test were designed to fail at around 7 kN, rock climbing anchors can vary greatly in strength. Geometry, rope length, and anchor strength will cause these results to vary. Stronger anchors will absorb more energy.

We cannot recommend the use of static rope for lead climbing configuration. Our simulations indicate that top point anchors may fail for static ropes with fall factors $FF>0.5$ and $m=90$ kg. Others maintain a fall factor of less than $FF<0.3$ for an 80kg mass and using new rope is acceptable. Frequently, climbers will place protection further apart than perceived necessary. In climbing with a static rope, this could be disastrous. More testing is needed to fully understand the risk of falling on static ropes.

Ice protection with strength ranges between 7 to 8 kN is unlikely to arrest a fall in any configuration with static rope.

ACKNOWLEDGEMENTS:

We would like to thank the National Mountain Rescue Association for supporting this project, Pigeon Mountain Industries, Sterling Rope, and Petzl for their contributions, the Albuquerque Academy School and Mike Shaa for use of their tower.

Thank you to our friends:

Albuquerque Mountain Rescue: Nick McKinley, Bill Scherzinger, Jason Williams

Ouray Mountain Rescue: Mark Miller

We would also like to thank our family members who helped or allowed us to work on this project.

We hope that this information will be useful to those who use rope at work and play that this information will be disseminated.

REFERENCES

¹ Moyer, Tom. ITRS 2006.

² http://en.petzl.com/petzl/frontoffice/static/EPI/index_en.jsp?Section=Sport

³ <http://www.uiaa.ch/web.test/visual/Safety/UIAA101DynamicRopes07-2004.pdf>

⁴ <http://www.uiaa.ch/web.test/visual/Safety/PictUIAA101-EN892DynamicRopes.pdf>

⁵ Beverly, J. Marc, M-PAS, Climbers Think: an On-Line Survey ITRS 2005.

⁶ J. Vogwell a, J.M. Minguez. The safety of rock climbing protection devices under falling loads. Engineering Failure Analysis 14 (2007) 1114–1123.

⁷ Luebben, Craig. How to Ice Climb (pp.143-158). Connecticut: The Globe Pequot Press, 1999.

⁸ http://mccammon.ucsd.edu/~adcock/mountaineering_glossary.html

⁹ http://www.gmanews.tv/everest/faq_glossary.htm

¹⁰ The Mountaineer, edited by Cox and Fulsaa. Mountaineering: The Freedom of the Hills 7th ed. (pg 263, 264) The Mountaineers Books, 2003.

¹¹ Beverly, J. Marc, M-PAS, Attaway, S. PhD, et al., Multi-point Pre-Equalized Anchoring Systems. ITRS 2005.

¹² Beverly, J. Marc, M-PAS, Attaway, S. PhD, Dynamic Shock Load Evaluation of Ice Screws: A Real-World Look. ITRS 2005.

¹³ Manning, T. Rescue System Mechanics, Interim Report. ITRS 2000.

¹⁴ Fox, Adam Materials testing of climbing equipment: debunking common myths and confirming truths. 2003. Fox Mountain Guides. www.foxmountainguides.com

¹⁵ UIAA Reference....insert here.

¹⁶ Beverly, J. Marc, M-PAS, Attaway, S. PhD. Hang ‘Em High: How Far Can You Trust Your Belay Device? ITRS 2005.

¹⁷ Attaway, S. W. and Weber, C, “Predicting Rope Impact Forces Using a Non-linear Force Deflection, ITRS 2002.

¹⁸ National Park Service Search and Rescue Manual. Basic Technical Rescue, 10th Ed. Pg 10. Revised March 2005.

¹⁹ Hohlrieder, Matthias, MD, Lutz, MartinMD, et al.. Pattern of Injury After Rock Climbing Falls Is Not Determined by Harness Type. Wilderness and Environmental Medicine. **18**, 30-35 (2007).